The Dissociative Recombination of Protonated Acrylonitrile, CH2CHCNH+, with Implications for Nitrile Chemistry in Dark Molecular Clouds and the Upper Atmosphere of Titan

Published in:
Astrophysical Journal

Queen's University Belfast - Research Portal:
Link to publication record in Queen's University Belfast Research Portal

THE DISSOCIATIVE RECOMBINATION OF PROTONATED ACRYLONITRILE, CH_2CHCNH^+, WITH IMPLICATIONS FOR THE NITRILE CHEMISTRY IN DARK MOLECULAR CLOUDS AND THE UPPER ATMOSPHERE OF TITAN

E. Vigren[1,2], M. Hamberg[1], V. Zhaunerchyk[1], M. Kamińska[1,3], R. D. Thomas[1], M. Larsson[1], T. J. Millar[4], C. Walsh[4],
and W. D. Geppert[1]
[1] Department of Physics, AlbaNova, Stockholm University, SE-10691 Stockholm, Sweden; wgeppert@hotmail.com
[2] Astrobiology Graduate School, Stockholm University, Stockholm, Sweden
[3] Institute of Physics, Jan Kochanowski University, Świętokrzyska 15, PL-25406 Kielce, Poland
[4] Astrophysics Research Centre, School of Mathematics and Physics, Queen's University Belfast, Belfast BT7 1NN, UK

ABSTRACT

Measurements on the dissociative recombination (DR) of protonated acrylonitrile, CH_2CHCNH^+, have been performed at the heavy ion storage ring CRYRING located in the Manne Siegbahn Laboratory in Stockholm, Sweden. It has been found that at ∼2 meV relative kinetic energy about 50% of the DR events involve only ruptures of X–H bonds (where X = C or N) while the rest leads to the production of a pair of fragments each containing two heavy atoms (alongside H and/or H_2). The absolute DR cross section has been investigated for relative kinetic energies ranging from ∼1 meV to 1 eV. The thermal rate coefficient has been determined to follow the expression $k(T) = 1.78 \times 10^{-6} (T/300)^{-0.80}$ cm^3 s^{-1} for electron temperatures ranging from ∼10 to 1000 K. Gas-phase models of the nitrile chemistry in the dark molecular cloud TMC-1 have been run and results are compared with observations. Also, implications of the present results for the nitrile chemistry of Titan's upper atmosphere are discussed.

Key words: ISM: clouds – ISM: molecules – methods: laboratory – molecular processes

1. INTRODUCTION

Dissociative recombination (DR) is a process in which a free electron is captured by a molecular cation forming a highly excited intermediate neutral state which subsequently releases the excess energy through decay into neutral fragments. In low-density plasmas that are cold enough to contain molecular ions, where low collision energies prevail and three-body reactions are unimportant, DR plays a crucial role in plasma neutralization. Storage rings, such as CRYRING (Stockholm) and TSR (Heidelberg) provide the opportunity to study the DR cross section at different well-defined interaction energies. CRYRING also allows one to establish the sets of fragments into which the highly excited intermediate molecule dissociates (Larsson 1997).

During the last few years a number of nitrile ions have been investigated at CRYRING (Geppert et al. 2004; Vigren et al. 2008). These studies were mainly motivated by the detection of these species in various extraterrestrial environments and the need for insight into their synthesis. In this paper we present an investigation into the DR of protonated acrylonitrile (vinylcyanide), CH_2CHCNH^+, including determination of the DR cross section, the thermal rate coefficient and the branching fractions.

Acrylonitrile (CH_2CHCN) was detected toward Sgr B2 by Gardner & Winnewisser (1975) and later also observed in the cold dark cloud TMC-1 by Matthews & Sears (1983). The molecule has recently been seen in the envelope of the carbon-rich star IRC+10216 (Agúndez et al. 2008). The protonated form of the molecule has been argued to exist in high abundances in the upper atmosphere of Titan based on a strong signal at $m/z = 54$ recorded by the ion-neutral-mass spectrometer (INMS) on board the *Cassini* spacecraft during a flyby on 2005 April 16 (Vuitton et al. 2006). The *Cassini* flyby and the associated analysis have truly rendered new insights about the chemistry in Titan's ionosphere. It has been shown that the nitrogen chemistry is more evolved than previously realized and in particular it has been discovered that the abundances of several protonated nitriles are much higher than predicted by pre-*Cassini* models (e.g., Keller et al. 1998). A better insight into the formation and destruction routes of these ions is important to improve chemical models of Titan's upper atmosphere (Vuitton et al. 2006, 2007).

Our investigation into the $CH_2CHCNH^+ + e^-$ reaction is also relevant to models of molecular clouds and circumstellar envelopes. Based on ion flow tube experiments (Petrie et al. 1991), which showed no detectable reactivity of CH_2CHCNH^+ with important interstellar neutral molecules (e.g., H_2, CO, O_2, and CH_4), Petrie et al. (1992) stated that electron recombination is the major loss process of this ion in the dark molecular cloud TMC-1. We have incorporated the results from the present study (and others) in gas-phase models aimed to simulate the chemical evolution of TMC-1. We present in Section 4.2 details about these models as well as obtained results.

Finally, the DR of CH_2CHCNH^+ is compared with previously studied nitrile ions, in particular $DCCCN^+$ and $DCCCND^+$.

2. EXPERIMENT

The experiments were performed at the heavy ion storage ring CRYRING. A detailed description of the experimental facility and procedure is available in the literature (Neau et al. 2000; Strömholm et al. 1996) and only the features relevant to the present studies will be discussed here. CH_2CHCNH^+ ions were produced from a mixture of acrylonitrile and H_2 in a hollow cathode discharge ion source, JIMIS (Peterson et al. 1998).

The ions were extracted from the source at 40 keV, mass selected by a bending magnet and injected into the storage ring, which has a circumference of 51.6 m. In the ring they were accelerated to 1.8 MeV by a radio frequency cavity. In one of the straight sections of the ring the ions were merged with a colinear beam of electrons in an electron cooler (see e.g., Danared et al. 2000). The continuously renewed electrons, whose velocity

could be controlled by tuning the cathode voltage of the electron cooler, had a low energy spread described by a flattened Maxwellian distribution in the interaction region (estimated transversal and longitudinal electron temperatures of 2 meV and 0.1 meV, respectively). Therefore heat was transferred, by means of Coulombic interaction, from the warmer ions to the electrons which decreased the phase space volume of the ions. However, due to the relatively high mass of the investigated ion, this cooling process was not particularly efficient and the purpose of the electrons was in essence only to serve as targets for the DR reactions. Prior to data acquisition from the DR reaction, the accelerated ion beam was stored in the ring for an extra 3.0 s which allowed ions produced in vibrationally excited states to relax by means of infrared photon emission. This was important for the validity of using our results in astrochemical models since vibrationally excited molecules/molecular ions are rare in cold dark molecular clouds. The neutral fragments produced by the DR reactions and by ion- rest gas collisions were not affected by the magnets in the ring (used to define the orbit of the ions) and left it tangentially in a straight line. At a distance of 3.85 m from the center of the interaction region they impinged on an energy sensitive ion-implanted silicon detector (IISD). A micro channel plate (MCP) detector located in another part of the ring was used to monitor signals arising from reactions between ions and residual gas versus time, the intensity of which being proportional to the ion current.

Further experimental details with regard to the DR cross section- and branching fraction measurements are presented in Sections 3.1 and 3.2, respectively.

3. DATA ANALYSIS

3.1. Determining the Cross Section and the Thermal Rate Coefficient for the DR of CH_2CHCNH^+

During the cross-section measurements, the cathode voltage of the electron cooler was scanned from a value corresponding to a relative kinetic energy (i.e., sum of the kinetic energies of the particles relative to the center of mass) of 1 eV, with the electrons being faster than the ions, down to a lower value, again corresponding to a relative kinetic energy of 1 eV, but now with the electrons being slower than the ions. The output signal from the IISD was amplified and monitored by a multichannel scaler (MCS), and so the number of counts versus storage time was recorded. By dividing each data point in the MCS spectrum by the number of experimental cycles and the length of the dwell time the count rate (dN/dt) could be obtained versus relative kinetic energy (in the cathode voltage scan a certain time corresponds to a certain relative kinetic energy). Signals recorded at collision energies close to 1 eV were (in the analysis) assumed to be completely dominated by counts arising from reactions between ions and residual gas molecules, since the DR cross section typically is very low at such interaction energies (see, e.g., Hellberg et al. 2005). An exponential decay function was fitted to these data points and this function was then subtracted from the MCS spectrum yielding a spectrum of pure DR events per second (dN_{DR}/dt) versus relative kinetic energy. The decay constant was similar to that of the exponential decay of the ion current as measured by the MCP detector which just records pure background events. The absolute ion current, I_{ion}, was monitored at the end of the acceleration phase by a capacitive pickup which was calibrated to an AC transformer (details are given by Paal et al. 2006). At this stage the proportionality of the ion current to the intensity of the

background signals was established. The electron current, I_e, was measured by a multimeter at the electron collector of the electron cooler.

The DR rate coefficient, α, is given in measured quantities as

$$\alpha = \frac{dN_{DR}}{dt} \frac{q^2 v_e v_{ion} \pi r_{e\text{-beam}}^2}{I_e I_{ion} l}, \qquad (1)$$

where dN_{DR}/dt is the DR count rate, q is the elementary charge, v and I denote velocities in the laboratory frame and currents, respectively, $r_{e\text{-beam}}$ is the radius of the electron beam and l is the length of the interaction region. The velocity of the electrons was determined from the cathode voltage of the electron cooler and corrected for the space charge effect (DeWitt et al. 1996). The radius of the electron beam is 2 cm (Danared et al. 2000) and the length of the colinear interaction region is 85 cm. DR reactions also occurred in the regions where the electrons were bent into and out of the ion beam by magnets. In these toroidal regions the beams were not parallel and hence the interaction energy was higher. A procedure, described by Lampert et al. (1996) to correct for signals arising from these regions was undertaken.

The DR cross section, $\sigma(E)$, versus interaction energy was obtained by dividing the rate coefficient by the electron velocity in the center-of-mass frame. At lower interaction energies the transversal energy spread of the electrons had to be taken into account and in this case the DR cross section versus interaction energy was extracted (see, e.g., Mowat et al. 1995) from the expression

$$\langle \sigma v_{rel} \rangle = \int v_{rel} f(v_{rel}) \sigma(v_{rel}) d^3 v_{rel}, \qquad (2)$$

where $f(v_{rel})$ is the relative velocity distribution. In the analysis only the transversal velocity spread of the electrons was considered since the estimated longitudinal velocity spread of the electrons and velocity spreads of the ions are much smaller. The absolute DR cross section for CH_2CHCNH^+ versus relative kinetic energy is presented in Figure 1. Over the energy range from ∼1 meV to ∼0.1 eV it is well fitted by the expression

$$\sigma(E) = (1.15 \pm 0.2) \times 10^{-15} \cdot E^{-1.29 \pm 0.02} \text{ cm}^2. \qquad (3)$$

For energies above 0.1 eV the cross section drops with increasing collision energy as ∼$E^{-1.6}$. The change of slope possibly occurs due to the opening of a new autoionization channel into a vibrationally excited state of the ion (see, e.g., Jensen et al. 1999). To find the thermal rate coefficient at a specific (electron) temperature the cross section was integrated over the isotropic Maxwellian electron speed distribution assumed to be present at that temperature

$$k(T) = \left(\frac{m_e}{2\pi k_B T}\right)^{3/2} \int_0^{\infty} v\sigma(v)e^{-m_e v^2/2k_B T} 4\pi v^2 dv, \qquad (4)$$

where m_e is the electron mass, k_B is Boltzmann's constant and v denote electron velocity. The thermal rate coefficient for the DR of CH_2CHCNH^+ was found to be well fitted by the function

$$k(T) = (1.78 \pm 0.3) \times 10^{-6} \cdot (T/300)^{-0.80 \pm 0.02} \text{ cm}^3 \text{ s}^{-1}. \quad (5)$$

This formula is valid up to about 1000 K.

For the DR cross section the systematical uncertainties (such as the electron beam radius, the length of the interaction region,
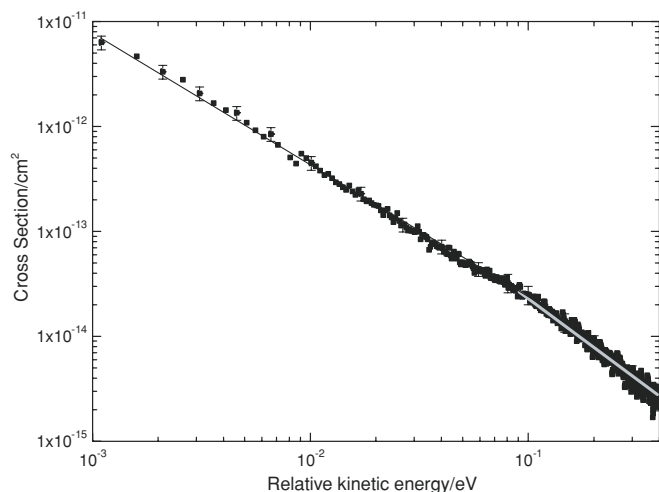
Figure 1. The absolute DR cross section vs. relative kinetic energy in the DR of CH$_2$CHCNH$^+$. The black line shows the best fit of the data for relative kinetic energies ranging from 1 meV to 0.1 eV with $\sigma = 1.15 \times 10^{-15} \cdot E^{-1.29}$ cm^2. Above 0.1 eV the cross section is best fitted by an $E^{-1.6}$ dependence indicated by the gray line.

Figure 2. The background-subtracted energy spectrum recorded at $\sim$2 meV relative kinetic energy between the electrons and the ions (grid inserted) for the DR of CH$_2$CHCNH$^+$.

Table 1
The Exoergic Channels in the Reaction CH$_2$CHCNH$^+$ + Electron

Channel	ΔH (eV)	Channel	ΔH (eV)
(6a) C$_3$H$_3$N + H	−5.4	(6l) CNH$_3$ + C$_2$H	−3.2
(6b) C$_3$H$_2$N + H$_2$	−5.2	(6m) CNH$_2$ + C$_2$H$_2$	−4.7
(6c) C$_3$H$_2$N + 2H	−0.7	(6n) HCN + C$_2$H$_3$	−5.0
(6d) C$_3$HN + H + H$_2$	−3.6	(6o) HCN + C$_2$H$_2$ + H	−3.4
(6e) C$_3$N + 2H$_2$	− 5.2	(6p) HCN + C$_2$H + H$_2$	−3.2
(6f) C$_3$N + 2H + H$_2$	− 0.7	(6q) CN + C$_2$H$_4$	−4.5
(6g) C$_2$H$_3$N + CH	−2.6	(6r) CN + C$_2$H$_2$ + H$_2$	−2.6
(6h) C$_2$H$_2$N + CH$_2$	−2.9	(6s) NH$_3$ + C$_3$H	−2.3
(6i) C$_2$HN + CH$_3$	−3.0	(6t) NH$_2$ + C$_3$H$_2$	−2.3
(6j) C$_2$N + CH$_4$	−4.5	(6u) NH + C$_3$H$_3$	−2.1
(6k) C$_2$N + CH$_3$ + H	0.0	(6v) N + C$_3$H$_4$	−2.7

Notes.
The listed energies refer to the rovibronic ground states of the species. Heats of formation have been taken from NIST Chemistry Webbook (2005) , Mayer et al. (1998), Meyer & Setser (1970), Lau & Ng (2006), and Lias et al. (1988).

the ion beam circumference) and statistical uncertainties (e.g., counts from DR events) sum to about 15%–20% in the lower energy range (below 0.1 eV) whereas the cross section in the higher energy range has larger uncertainties, mainly due to the poorer statistics. It should be noted that the high uncertainties in the higher energy range have no major effect on the uncertainty in the thermal rate coefficient below 1000 K.

3.2. Determining the Branching Fractions in the DR of CH$_2$CHCNH$^+$

The branching fractions were investigated at $\sim$2 meV relative kinetic energy. The amplified signals from the detector were now recorded by a multichannel analyzer (MCA) thus recording counts versus kinetic energy of the DR fragments in the lab frame (a pulse height spectrum). To account for signals arising from reactions between the ions and the residual gas the same measurements were repeated at 1 eV, where, as mentioned, essentially all counts are due to non-DR processes. The spectra were normalized according to the intensity of the ion beam as recorded by the MCP detector.

At $\sim$0 eV relative kinetic energy the DR of CH$_2$CHCNH$^+$ can lead to the products listed in entries (6a)–(6v) in Table 1. The given exoergicities refer to the ground states of both the ion and the neutral products (with respect to most stable isomer).

In (6a)–(6f) the four heavy atoms remain covalently bonded and only hydrogen atoms are detached whereas in (6g)–(6k) a carbon atom is detached from the other three heavy atoms. The reaction channels (6l)–(6r) lead to two heavy fragments each containing two heavy atoms and in the channels (6s)–(6v) the carbon–nitrogen bond is broken.

The products originating from a single recombination event hit the detector on a time scale much shorter than the integration time of the detector, and so produce a signal proportional to the full mass of the DR products. This makes it impossible to distinguish between events originating from the different dissociation channels. To solve this problem a grid with a transmission probability of $P = 0.297 \pm 0.015$ was inserted in front of the detector. Since a part of the particles were stopped by the grid, the recorded pulse height spectrum showed a series
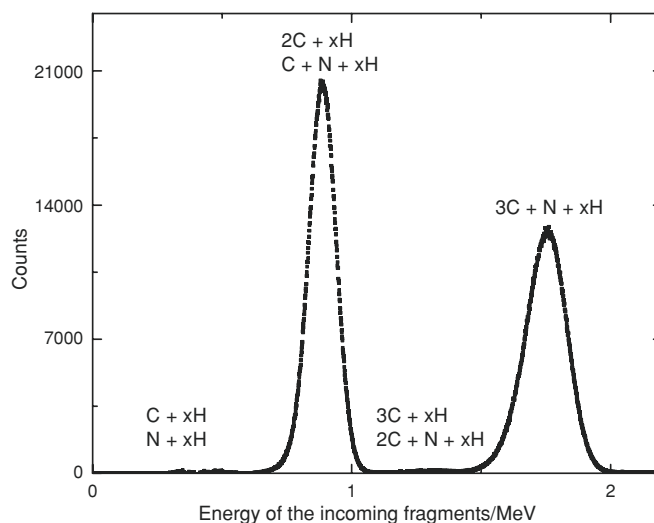
of peaks corresponding to the total mass of the particles that passed through the grid. After background subtraction the pure DR spectrum at $\sim$2 meV relative kinetic energy was obtained, and this is shown in Figure 2.

Analysis of the data plotted in Figure 2 showed that the resolution of the detector was only sufficient to resolve fragments differing in mass by at least one heavy atom. A detailed analysis of the branching fractions could not therefore be performed and only information about the fragmentation of bonds between the heavy atoms could be gained.

Consider as an example (6r) in which the DR leads to CN + C$_2$H$_2$ + H$_2$. It is not possible for this channel to contribute to the peak labeled C + xH, N + xH (see Figure 2) since the channel does not produce a product containing only one heavy atom. Similarly the peak labeled 3C + xH, 2C + N + xH cannot originate from (6r) either. Conversely, (6r) can give rise to the peak labeled 2C + xH, C + N + xH. This happens if one of the heavy fragments is stopped by the grid while the other one passes. The probability for this to occur is $2P(1-P)$. Finally (6r) can contribute to the peak labeled 3C + N + xH given that both heavy fragments pass through the grid, which has a probability of P^2. The following equation system can be established in

Table 2
The Branching Fractions in the Dissociative Recombination of CH_2CHCNH^+

Fragmentation		Percentage
(6a--6f)	$C_3NH_x + yH + wH_2$	50% ± 4%
(6l–6r)	$C_2H_x + CNH_y + zH + wH_2$	49% ± 4%
(6g–6k) and (6s-6v)	$C_3H_x + NH_y$; $C_2NH_x + CH_y + zH$	1% ± 1%

Note. For each line $x + y + z + 2w = 4$.

analogy with the example given above:

$$\begin{bmatrix} I(C + xH, N + xH) \\ I(2C + xH, C + N + xH) \\ I(3C + xH, 2C + N + xH) \\ I(3C + N + xH) \end{bmatrix}$$
$$= \begin{bmatrix} 0 & P(1-P) & 0 \\ 0 & 0 & 2P(1-P) \\ 0 & P(1-P) & 0 \\ P & P^2 & P^2 \end{bmatrix}$$
$$\times \begin{bmatrix} N(6a-6f) \\ N(6g-6k, 6s-6v) \\ N(6l-6r) \end{bmatrix}. \quad (6)$$

In Equation (6) I denotes the intensities of the peaks in Figure 2 and N the number of reactions of a particular type. The first and the third rows in the equation system are identical so one of these can be disregarded yielding an equation system with three equations and three unknowns. Solving this system gives the values of $N(6a–6f)$, $N(6g–6k, 6s–6v)$ and $N(6l–6r)$ and by normalizing the results to the total number of reactions yield the branching fractions presented in Table 2. Analysis of these results shows that the DR of CH_2CHCNH^+ is dominated by reactions in which the heavy atom structure is preserved and by reactions producing two fragments with a pair of heavy atoms each. The errors presented in Table 2 are mainly due to the uncertainty in the transmission probability of the grid.

4. DISCUSSION

4.1. The Dissociative Recombination of CH_2CHCNH^+

The extent to which isomers could have been present during the experiment must first of all be discussed. It has been shown theoretically that acrylonitrile is protonated preferably at the nitrogen atom (Wu & Glaser 2005). Proton attachments on C1 and C2 (with C1 being the carbon atom farthest away from the N atom) are less exoergic by 177 and 243 kJ mol^{-1}, respectively. Some contributions to the ion beam by contamination from ionized acrylonitrile, containing one deuterium atom, ^{13}C atom or ^{15}N atom, is expected to have occurred. Assuming natural isotope abundances of H, C, and N the probability for ionized acrylonitrile to have a mass higher than 53 amu is only ∼3.7%. Mass spectra were recorded before and after the experiment giving currents for $m/z = 53$ similar to those for $m/z = 54$. Thus, the contamination of ionized acrylonitrile containing one deuterium atom, ^{13}C atom or ^{15}N atom should have been below 4%.

To the best of our knowledge this is the first experimental investigation into the DR of CH_2CHCNH^+. Nevertheless, our results can be compared with results from DR experiments of two other nitrile ions, DCCCN$^+$ and DCCCND$^+$, both of which possess a CCCN chain. The thermal rate coefficients for both DCCCN$^+$ and DCCCND$^+$ (Geppert et al. 2004) follow the expression $k(T) = 1.5 \times 10^{-6}(T/300)^{-0.6}$ cm^3 s^{-1}, which at 300 K

is quite similar to the value of 1.78×10^{-6} cm^3 s^{-1} reported here for the DR of CH_2CHCNH^+. The temperature dependences are, however, notably different, with $k(T)$ proportional to $(T/300)^{-0.6}$ for the DR of DCCCN$^+$ and DCCCND$^+$ and to $(T/300)^{-0.8}$ for the DR of CH_2CHCNH^+. Therefore, the rate coefficient at 10 K for the DR of CH_2CHCNH^+ is more than twice as large as compared to those of DCCCN$^+$ and DCCCND$^+$.

The branching fractions reported here for the DR of CH_2CHCNH^+ show striking similarities to those measured for the DR of DCCCND$^+$, with those channels which involve the detachment of only D/H atoms accounting for about half of the DR events and reactions yielding two heavy fragments containing two heavy atoms each accounting for the other half of the DR events. Furthermore, in the DR of DCCCN$^+$, these types of break up dominate (∼44% conservation of the heavy atom structure and ∼48% giving two heavy fragments with two heavy atoms each) but reactions do exist in which a fragment with one heavy atom is produced (∼8%). The somewhat lower fraction of reactions in which the CCCN backbone is conserved in the DR of DCCCN$^+$ might reflect the fact that there is only one D-atom in this system and that only one DR reaction which preserves the CCCN chain exists.

The effect of internal excitation of the reacting ion on the reported rate coefficient is an important subject to discuss. Although the utilized ion source, JIMIS, operates under a fairly high pressure (∼kPa) and originally was designed to produce vibrationally cold ions by collisional quenching (Peterson et al. 1998) it cannot be completely ruled out that some of the ions extracted from the source were vibrationally excited in the beginning of storage in the present experiment. One could assume, as is the case for the neutral molecule CH_2CHCN (Popov et al. 1969), that all vibrational modes of CH_2CHCNH^+ are IR active and expect that the storage time of 4 s should have been sufficient to reach the $v = 0$ level of all modes. Nevertheless, this cannot be taken for granted as it for example has been shown that the lifetimes of vibrationally excited states ($v = 1, 2, 3$) in the (IR active) bending mode of DCO$^+$ exceed 4 s (Wester et al. 2002). For other molecular ions (for which vibrational lifetimes have been investigated) such as N$_2$H$^+$, N$_2$D$^+$ (Heninger et al. 2003), H$_2$O$^+$ and D$_2$O$^+$ (Heninger et al. 1994) to mention a few, the reported total vibrational lifetimes are in the range of a few to a few hundreds of milliseconds. Existence of long-living vibrational excited states of IR-active modes is therefore probably quite rare. It is somewhat difficult to discuss the effect of vibrational excitation on the DR rate coefficient for CH_2CHCNH^+ since this requires insight into the very complex potential surfaces involved in the reaction. In the case of H$_2^+$ the DR rate coefficient is much higher for vibrationally excited ions than for ions in the ground state. This is due to the poor overlap between the dissociative doubly excited state (through which dissociation occurs) and the $v = 0$ ground state of H$_2^+$ (see, e.g., Zhaunerchyk et al. 2007). For other ions, such as O$_2^+$, vibrational excitation appears less important and only brings about a slight decrease of the DR thermal rate coefficient (Petrignani et al. 2005). In summary, we expect that the CH_2CHCNH^+ ions were vibrationally thermalized to the ambient temperature (300 K) during the count rate measurements and that the presence of some vibrationally excited ions do not have a severe effect on the reported rate coefficient for an ion of comparatively low symmetry such as CH_2CHCNH^+.

The effect of rotational excitation on the DR rate coefficient has been investigated for H$_3^+$. It has been found from CRYRING

Table 3
Changes Made to Models 1–9 with Respect to the Original Model (Woodall et al. 2007)

Reaction	Action	Rate Coefficient ($cm^3\ s^{-1}$)
(8a) $N_2H^+ + e^- \rightarrow N_2 + H$	Changed	$k(T) = 1.53 \times 10^{-7}\ (T/300)^{-0.92}$
(8b) $N_2H^+ + e^- \rightarrow NH + N$	Changed	$k(T) = 1.70 \times 10^{-8}\ (T/300)^{-0.92}$
(8c) $CH_3CNH^+ + e^- \rightarrow CH_3CN + H$	Changed	$k(T) = 2.64 \times 10^{-7}\ (T/300)^{-0.69}$
(8d) $CH_3CNH^+ + e^- \rightarrow CH_2CN + 2H$	Added reaction	$k(T) = 2.64 \times 10^{-7}\ (T/300)^{-0.69}$
(8e) $CH_3CNH^+ + e^- \rightarrow CH_2CN + H_2$	Removed reaction	
(8f) $CH_3CNH^+ + e^- \rightarrow CH_3 + HNC$	Added reaction	$k(T) = 1.42 \times 10^{-7}\ (T/300)^{-0.69}$
(8g) $CH_3CNH^+ + e^- \rightarrow CH_2 + HCN + H$	Added reaction	$k(T) = 1.42 \times 10^{-7}\ (T/300)^{-0.69}$
(8h) $H_4C_3N^+ + e^- \rightarrow CH_2CHCN + H$	Changed to	$k(T) = 8.90 \times 10^{-7}\ (T/300)^{-0.80}$
(8i) $H_4C_3N^+ + e^- \rightarrow HC_3N + H_2 + H$	Removed reaction	
(8j) $H_4C_3N^+ + e^- \rightarrow C_2H_2 + HCN + H$	Added reaction	$k(T) = 4.45 \times 10^{-7}\ (T/300)^{-0.80}$
(8k) $H_4C_3N^+ + e^- \rightarrow C_2H_3 + CN + H$	Added reaction	$k(T) = 4.45 \times 10^{-7}\ (T/300)^{-0.80}$
(8l) $CN + C_2H_4 \rightarrow CH_2CHCN + H$	Changed	$k(T) = 2.67 \times 10^{-10}\ (T/300)^{-0.69}\ e^{-31/T}$
(8m) $CN + C_2H_4 \rightarrow C_2H_3 + HCN$	Removed reaction	

measurements (McCall et al. 2004; Sundström et al. 1994) that the thermal rate coefficient for cold H_3^+ ions ($T_{rot} \sim 30$ K; ions produced in a supersonic expansion ion source) was about 40% lower than for hot ions (T_{rot} possibly a few 1000 K) produced in a hot filament ion source and stored for 8 s prior to data acquisition. The branching fractions of the $H_2 + H$ and the $H + H + H$ channel were also slightly affected by the rotational temperature with that of the dominating three-body channel decreasing from ~ 0.75 (Datz et al. 1995; "hot" ions) to 0.64 ± 0.05 (McCall et al. 2004, "cold" ions). However, conclusions on the rotational dependence of the DR rate coefficient and branching ratios of CH_2CHCNH^+ from the data for H_3^+ will not be straightforward. Most importantly, H_3^+ lacks a permanent dipole moment and its rotational temperature does not change much during usual storage times. For example, even after 40 s of electron cooling and storage in the Test Storage Ring in Heidelberg, the rotational temperature of H_3^+ (produced in a "hot" gas discharge ion source) was still ~ 3500 K (Strasser et al. 2002). Whereas the neutral molecule, CH_2CHCN, has been reported to have a dipole moment of $\mu_e \sim 3.88$ D (Hurdis & Smith 1943) we have not been able to find the dipole moment of CH_2CHCNH^+ in the literature. We assume, however, based on reports for various other nitriles in their neutral and protonated form ($\mu_e(CH_3CN) \sim 3.92$ D (Gadhi et al. 1995), $\mu_e(CH_3CNH^+) \sim 1.04$ D (Botschwina 2000), $\mu_e(HCCCN) \sim 3.73$ D (DeLeon & Muenter 1985), $\mu_e(HCCCNH^+) \sim 1.61$ D (Botschwina & Heyl 1999)) the dipole moment of CH_2CHCNH^+ to be in the vicinity of 1 Debye. Therefore, the storage time employed in the present study (4–6 s), should allow sufficient relaxation by interaction with the blackbody field from the vacuum tube to a rotational distribution nearly corresponding to a temperature of 300 K.

4.2. Gas-phase Models of Nitrile Chemistry in TMC-1

We have modeled the chemical evolution of several nitriles in the molecular cloud, TMC-1, using the dipole enhanced version of the latest release of the UMIST Database for Astrochemistry (see www.udfa.net and Woodall et al. 2007). The models were run with the physical parameters appropriate for cold, dense molecular clouds, $T = 10$ K, $n(H_2) = 10^4$ cm^{-3} and $A_v = 15$ mag and we employed the low-metal initial elemental abundances of He, C^+, N, O, S^+, Si^+, Na^+, Mg^+, Fe^+, P^+, F, and Cl^+ typically used for TMC-1 as listed in Table 8 of Woodall et al. (2007).

We have modified the reaction database according to recent CRYRING results as well as with respect to a few older results from various experimental techniques. The list of common

changes made to all models is presented in Table 3. The rate coefficients for the DR reactions of N_2H^+, CH_3CNH^+, and CH_2CHCNH^+ were changed. The product distribution in the DR of N_2H^+ has been investigated by Molek et al. (2007) and reinvestigated at CRYRING (unpublished data). The latest results agree that $N_2 + H$ is the dominant channel. The thermal rate coefficient used for the DR of N_2H^+ is derived from Adams et al. (1984). The branching fractions used for the DR of CH_3CNH^+ and $H_4C_3N^+$ (CH_2CHCNH^+) are ambiguous since experimental limitations only allowed investigation into the distribution of the heavy atoms (as discussed earlier and Vigren et al. 2008); (8e) was replaced by (8d) since the former requires an extensive rearrangement to produce an H_2 molecule alongside CH_2CN. In the DR of CH_2CHCNH^+ we employed an optimistic CH_2CHCN production, i.e., all reactions only involving detachments of hydrogen atoms were assumed to lead to CH_2CHCN. The actions taken for reactions (8l) and (8m) are motivated by results from Choi et al. (2004), Balucani et al. (2000), and Sims et al. (1993).

We ran nine different models. The difference between the models was the choice of rate coefficients for the radiative association reactions $CH_3^+ + HCN \rightarrow CH_3CNH^+$ (8n) and $CH_3^+ + HNC \rightarrow CH_3CNH^+$ (8o). The former reaction (8n) has been investigated both theoretically (Bates 1983) and experimentally (Anicich et al. 1995) with large differences in the rate coefficients (9.0×10^{-9} and 2.0×10^{-10} cm^3 s^{-1} at 300 K, respectively). It is not definite that the initial product formed in the association, CH_3NCH^+, will radiatively stabilize into CH_3CNH^+, although such arguments have been put forward (e.g., DeFrees et al. 1985) partly as an explanation to the low CH_3NC/CH_3CN ratio observed in TMC-1 (Irvine & Schloerb 1984). The theoretical value is employed in the model by Woodall et al. (2007). The reaction (8o) is not included in earlier models but could be important due to the relatively high HNC abundance observed in TMC-1. Table 4 summarizes the rate coefficients used for (8n) and (8o) in the different models.

The chemical age of TMC-1 (where time = 0 roughly refers to the time when the size and density of the object are such that cosmic rays replace interstellar UV photons as the dominant source of ionization deep inside the cloud) is not well established. However, comparisons of molecular observations with time-dependent chemical models suggest that the chemistry has not yet reached steady state and indicates a cloud age of approximately 10^5 years (see e.g., Pratap et al. 1997; Smith et al. 2004). We present abundances (relative to the abundance of H_2) of several nitriles which have been

Table 4
Rate Coefficients Applied in Model 1–9 for the Reactions (8n) $CH_3^+ + HCN \rightarrow CH_3CNH^+$ and (8o) $CH_3^+ + HNC \rightarrow CH_3CNH^+$

Rates Used for 8o (cm^3 s^{-1})	Rates Used for 8n (cm^3 s^{-1})		
	0	2.0×10^{-10} $(T/300)^{-0.50}$	9.0×10^{-9} $(T/300)^{-0.50}$
0	Model 1	Model 2	Model 3
2.0×10^{-10} $(T/300)^{-0.50}$	Model 4	Model 5	Model 6
9.0×10^{-9} $(T/300)^{-0.50}$	Model 7	Model 8	Model 9

Table 5
Comparison of Observed Abundances Relative to H$_2$ and Model Predictions At *Time* = 10^5 years for TMC-1, Each Entry in the Table Should be Multiplied by 10^{-9}

Species	Observed	Woodall et al. (2007)	Model 1	Model 2	Model 3	Model 4	Model 5	Model 6	Model 7	Model 8	Model 9
CN	30[a]	23	22	22	22	22	22	22	22	22	22
HCN	20[a]	40	44	44	41	44	44	41	44	44	41
HNC	20[a]	31	32	32	32	32	32	32	30	30	30
C$_3$N	0.8[b]	0.56	0.55	0.55	0.56	0.55	0.55	0.56	0.55	0.55	0.56
CH$_2$CN	6[b]	0.22	0.022	0.024	0.13	0.023	0.026	0.13	0.098	0.10	0.20
HC$_3$N	16[c]	5.8	3.6	3.6	4.8	3.6	3.6	4.8	4.4	4.5	5.6
CH$_3$CN	0.8[a]	1.6	0.11	0.13	0.92	0.13	0.15	0.93	0.70	0.71	1.5
CH$_2$CHCN	1[b]	0.00035	0.0014	0.0014	0.0014	0.0014	0.0014	0.0014	0.0014	0.0014	0.0013
HC$_5$N	5[b]	0.89	0.88	0.88	0.89	0.88	0.88	0.89	0.89	0.89	0.89
HCNH$^+$	2[a]	0.21	0.23	0.23	0.22	0.23	0.23	0.22	0.22	0.22	0.21

Notes.
[a] Ohishi et al. (1992).
[b] Ohishi & Kaifu (1998).
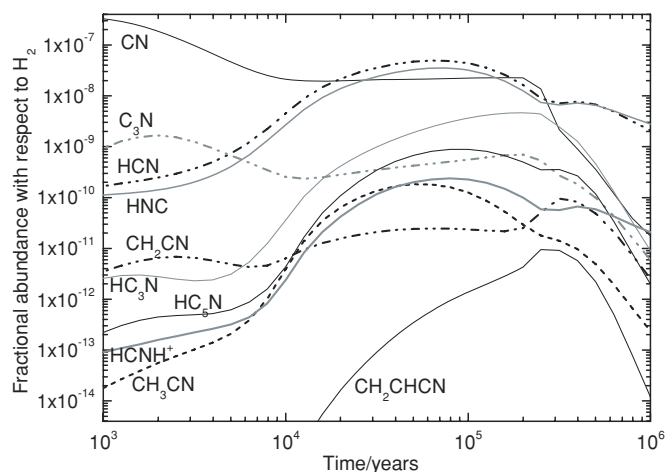[c] Takano et al. (1998).

Figure 3. The chemical evolution of selected nitrogen bearing species in TMC-1 as calculated by Model 4.

observed in TMC-1 (CN, HCN, HNC, C$_3$N, CH$_2$CN, HC$_3$N, CH$_3$CN, CH$_2$CHCN, HC$_5$N, and HCNH$^+$) as well as predicted abundances at 10^5 years from Model 1–9 and from the original model by Woodall et al. (2007) in Table 5.

The pure gas-phase models all give reasonable agreement with observations (within a factor of 10) at 10^5 years for CN, HCN, HNC, C$_3$N, HC$_3$N, CH$_3$CN, HC$_5$N, and HCNH$^+$. The calculated abundance of CH$_2$CN is sensitive to the choice of rate coefficients for (8n) and (8o) and varies from being a factor of ∼270 (Model 1) to a factor of ∼30 (Model 9) lower than observed. Even though using the most optimistic production rate of CH$_2$CHCN (given by our investigation on the DR of CH$_2$CHCNH$^+$) the abundance of CH$_2$CHCN is a factor of ∼700 lower than the observed value in Models 1–9. Figure 3 shows the chemical evolution of the ten listed species as a function of time as predicted by Model 4.

From Figure 3, it can be seen that according to Model 4 the peak abundance of CH$_2$CHCN (and CH$_2$CN) occurs at about time = 3×10^5 years. At this point the calculated fractional abundance of acrylonitrile is about seven times higher than at time = 1×10^5 years. It should be noted that the results presented in Table 5 are not much affected by the choice of rate coefficients used for (8a) and (8b).

4.3. The Formation of CH$_2$CHCN in Dark Molecular Clouds, a Mystery

The discrepancy between the modeled and observed abundances of CH$_2$CHCN in TMC-1 is large and reflects the absence of important production routes for CH$_2$CHCN in the models. Grain surface reactions, such as repeated hydrogenation of HC$_3$N with subsequent desorption, could be one such mechanism for the production of CH$_2$CHCN. Such a formation route was suggested by Blake et al. (1987) to explain the *absence* of CH$_2$CHCN and CH$_3$CH$_2$CN (propionitrile) in the cold ridge of the Orion molecular cloud and the *presence* of these molecules in the hot core of the same cloud. In the hot core, the abundance of CH$_3$CH$_2$CN was reported to be about 5.5 times higher than the abundance of CH$_2$CHCN (Blake et al. 1987). However, Minh & Irvine (1991) reported a non-detection of CH$_3$CH$_2$CN in TMC-1 and derived an *upper limit* for its abundance to be a factor of 2.5 lower than the abundance of CH$_2$CHCN. They argue that the non-detection of CH$_3$CH$_2$CN in TMC-1 is an indication of a gas-phase production route for CH$_2$CHCN in this cloud. If CH$_2$CHCN were formed on grain surfaces and desorbed (by whatever mechanism), CH$_3$CH$_2$CN should be detectable as well. This is because firstly, grain surface molecules tend to be saturated, meaning that CH$_3$CH$_2$CN should be more abundant than CH$_2$CHCN on grains, and secondly, the masses of the molecules only differ by two hydrogen atoms implying that the energy required for desorption of these two molecules should not be significantly different (Minh & Irvine 1991).

With all of these contradictory observations it seems like we have encountered a dead end. On one hand the non-detection of CH_3CH_2CN in TMC-1 points toward a gas-phase production of CH_2CHCN but on the other hand the pure gas-phase models under-predict the abundance of CH_2CHCN by a factor of $\sim$700. Due to the relatively high abundance of HNC observed in TMC-1 we encourage theoretical investigations of reactions involving this molecule. Reliable data for many HNC reactions (including the rate for 8o) lack in the models presented here. An example of an interesting ion neutral reaction, which is not included in our models but is exoergic and could potentially lead to protonated acrylonitrile, is the reaction between HNC and $C_2H_4^+$.

4.4. Implications for Titan's Upper Atmosphere

The signal at $m/z = 54$ measured by the INMS on the Cassini spacecraft was among the strongest signals detected ($\sim$100 cm^{-3}) during the Titan flyby labeled T5 reaching 1027 km above the surface at closest approach. This signal was attributed to CH_2CHCNH^+ mainly due to the high proton affinity of CH_2CHCN (Vuitton et al. 2006). The hydrocarbon ion $C_4H_6^+$ which also has $m/z = 54$ was deemed unlikely to contribute significantly to the signal since this radical cation is very reactive and should be destroyed quickly by proton transfer (Vuitton et al. 2006). The formation of nitriles in Titan's upper atmosphere is triggered by the destruction of the main components N_2 and CH_4 into atomic and molecular ions as well as excited atoms and molecules, which in turn can react to build up more complex molecules. Breaking the strong triple bond of N_2 requires an energy of $\sim$9.8 eV (Frost & McDowell 1956) and therefore dissociation reactions of N_2 are rare at low altitudes of Titan's atmosphere to which extreme UV radiation and magnetospheric electrons from Saturn seldom reach. This implies that the formation of complex nitrogen-bearing species, such as nitriles, mostly occur in the upper atmosphere of Titan, above $\sim$1000 km (Vuitton et al. 2007, see also references therein). Nitriles can follow different chemical pathways subsequent to their formation and insight into the competition between different chemical reactions in Titan's upper atmosphere is necessary for an understanding of nitrogen chemistry at all levels of the atmosphere (Vuitton et al. 2006, 2007). They can, for example, be lost by the sequence of protonation followed by DR. Alternatively, they can diffuse downward and polymerize and contribute to the formation of aerosols which are responsible for the orange haze of Titan.

The production of CH_2CHCNH^+ in Titan's atmosphere is believed to proceed mainly via the reaction CN + $C_2H_4 \rightarrow CH_2CHCN$ + H followed by protonation of CH_2CHCN. Due to the high proton affinity of CH_2CHCN (784.7 kJ mol^{-1}, Hunter & Lias 1998) it follows that CH_2CHCNH^+ on the one hand is readily produced from CH_2CHCN and on the other hand is quite stable toward proton transfer reactions. The main destruction mechanism of CH_2CHCNH^+ is therefore probably DR (Vuitton et al. 2007). Our results for this reaction indicate that acrylonitrile molecules, lost by protonation in Titan's upper atmosphere, can be significantly recycled by DR. It remains to be seen what explicit implications our results will have on chemical models of Titan's upper atmosphere.

5. CONCLUSIONS

The dissociative recombination of CH_2CHCNH^+ has been investigated at CRYRING. The reaction has a thermal rate coefficient of 1.78×10^{-6} $(T/300)^{-0.80}$ cm^3 s^{-1}. The highly

excited intermediate molecule preserves its heavy atom structure in about 50% of the reactions with only X–H bonds being broken (X = C or N). In the remaining $\sim$50% we observed a break of the second C–C bond leading to two heavy fragments containing two heavy atoms each. Channels yielding a fragment containing one heavy atom have been shown to be negligible (0%–2%). Both the thermal rate coefficient and the branching fractions are comparable with results reported for the DR of DCCCND$^+$ and DCCCN$^+$. Gas-phase models have been run for the dark molecular cloud TMC-1 and predicted abundances of different nitrogen bearing molecules have been compared with observed values. The agreement is reasonably good in general but the fractional abundance of acrylonitrile is $\sim$700 times less than its observed value. Our measurements also show that acrylonitrile molecules that are lost by protonation in the upper atmosphere of Titan can be extensively recycled by DR.

REFERENCES

Adams, N. G., Smith, D., & Alge, E. 1984, J. Chem. Phys., 81, 1778

Agúndez, M., Cernicharo, J., Pardo, J. R., Fonfría Expósito, J. P., Guélin, M., Tenenbaum, E. D., Ziurys, L. M., & Apponi, A. J. 2008, Astrophys. Space Sci., 313, 229

Anicich, V. G., Sen, A. D., Huntress, W. T., & McEwan, M. J. 1995, J. Phys. Chem., 102, 3256

Balucani, N., Asvany, O., Chang, A. H. H., Lin, S. H., Lee, Y. T., & Kaiser, R. I. 2000, J. Chem. Phys., 113, 8643

Bates, D. R. 1983, ApJ, 270, 564

Blake, G. A., Sutton, E. C., Masson, C. R., & Phillips, T. G. 1987, ApJ, 315, 621

Botschwina, P. 2000, J. Mol. Spectrosc., 203, 203

Botschwina, P., & Heyl, A. 1999, Mol. Phys., 97, 209

Choi, N., Blitz, M. A., McKee, K., Pilling, M. J., & Seakins, P. W. 2004, Chem. Phys. Lett., 384, 68

Danared, H., et al. 2000, Nucl. Instrum. Methods Phys. Res. A., 441, 123

Datz, S., Sundström, G., Biedermann, C., Broström, L., Danared, H., Mannervik, S., Mowat, J. R., & Larsson, M. 1995, Phys. Rev. Lett., 74, 896

DeFrees, D. J., McLean, A. D., & Herbst, E. 1985, ApJ, 293, 236

DeLeon, R. L., & Muenter, J. S. 1985, J. Chem. Phys., 82, 1702

DeWitt, D. R., Schuch, R., Gao, H., Zong, W., Asp, S., & Biedermann, C. 1996, Phys. Rev. A, 53, 2327

Frost, D. C., & McDowell, C. A. 1956, Proc. R. Soc. A, 236, 278

Gadhi, J., Lahrouni, A., Legrand, J., & Demaison, J. 1995, J. Chim. Phys., 92, 1984

Gardner, F. F., & Winnewisser, G. 1975, ApJL, 195, 127

Geppert, W. D., et al. 2004, ApJ, 613, 1302

Hellberg, F., et al. 2005, J. Chem. Phys., 122, 224314

Heninger, M., Lauvergnat, D., Lemaire, J., Boissel, P., Mauclaire, G., & Marx, R. 2003, Int. J. Mass. Spectrosc., 223–224, 669

Heninger, M., Lemaire, J., Mauclaire, G., Fenistein, S., Jullien, S., & Marx, R. 1994, J. Chem. Phys., 101, 1923

Hunter, E. P., & Lias, S. G. 1998, J. Phys. Chem. Ref. Data, 27, 413

Hurdis, E. C., & Smith, C. D. 1943, J. Am. Chem. Soc., 65, 89

Irvine, W. M., & Schloerb, F. P. 1984, ApJ, 282, 516

Jensen, M. J., Bilodeau, R. C., Heber, O., Pedersen, H. B., Safvan, C. P., Urbain, X., Zajfman, D., & Andersen, L. H. 1999, Phys. Rev. A, 60, 2970

Keller, C. N., Anicich, V. G., & Cravens, T. E. 1998, Planet. Space Sci., 46, 1157

Lampert, A., Wolf, A., Habs, D., Kettner, J., Kilgus, G., Schwalm, D., Pindzola, M. S., & Badnell, N. R. 1996, Phys. Rev. A, 53, 1413

Larsson, M. 1997, Annu. Rev. Phys. Chem., 48, 151
Lau, K. C., & Ng, C. Y. 2006, Chin. J. Chem. Phys., 19, 29
Lias, S. G., Bartmess, J. E., Liebman, J. F., Holmes, J. L., Levin, R. D., & Mallard, W. G. 1988, J. Phys. Chem. Ref.Data, 17, 1
Matthews, H. E., & Sears, T. J. 1983, ApJ, 272, 149
Mayer, P. M., Parkinson, C. J., Smith, D. M., & Radom, L. 1998, J. Chem. Phys., 108, 604
McCall, B. J., et al. 2004, Phys. Rev. A, 70, 052716
Meyer, J. A., & Setser, D. W. 1970, J. Phys. Chem., 74, 3452
Minh, Y. C., & Irvine, W. M. 1991, Astrophys. Space Sci., 175, 165
Molek, C. D., McLain, J. L., Poterya, V., & Adams, N. G. 2007, J. Phys. Chem., 111, 6760
Mowat, J. R., Danared, H., Sundström, G., Carlsson, M., Andersen, L. H., Vejby-Christensen, L., af Ugglas, M., & Larsson, M. 1995, Phys. Rev. Lett., 74, 50
Neau, A., et al. 2000, J. Chem. Phys., 113, 1762
NIST Chemistry Webbook 2005, NIST Standard Reference Database 69 (Gaithersburg, MD: National Institute of Standards and Technology)
Ohishi, M., Irvine, W. M., & Kaifu, N. 1992, in Proc. IAU Symp. 150, Astrochemistry of Cosmic Phenomena, ed. P. D. Singh (Dordrecht: Kluwer), 171
Ohishi, M., & Kaifu, N. 1998, Faraday Discuss., 109, 205
Paal, A., Simonsson, A., Dietrich, J., & Mohos, I. 2006, in Proc. EPAC 2006, European Particle Accelerator Conference, Edinburgh, 2006, The European Physical Society Accelerator Group (EPS-AG), 1196
Peterson, J. R., et al. 1998, J. Chem. Phys., 108, 1978

Petrie, S., Chirnside, T. J., Freeman, C. G., & McEwan, M. J. 1991, Int. J. Mass Spectrom., 107, 319
Petrie, S., Freeman, C. G., & McEwan, M. J. 1992, MNRAS, 257, 438
Petrignani, A., Cosby, P. C., Hellberg, F., Thomas, R. D., Larsson, M., & van der Zande, W. J. 2005, J. Chem. Phys., 122, 014302
Popov, E. M., Yakovlev, I. P., & Kogan, G. A. 1969, Theor. Exp. Chem., 3, 91
Pratap, P., Dickens, J. E., Snell, R. L., Miralles, M. P., Bergin, E. A., Irvine, W. M., & Schloerb, F. P. 1997, ApJ, 486, 862
Sims, I. R., Queffelec, J.-L., Travers, D., Rowe, B. R., Herbert, L. B., Karthauser, J., & Smith, I. W. M. 1993, Chem. Phys. Lett., 211, 461
Smith, I. W. M., Herbst, E., & Chang, Q. 2004, MNRAS, 350, 323
Strasser, D., Lammich, L., Kreckel, H., Krohn, S., Lange, M., Naaman, A., Schwalm, D., Wolf, A., & Zajfman, D. 2002, Phys. Rev. A, 66, 032719
Strömholm, C., Semaniak, J., Rosén, S., Danared, H., Datz, S., van der Zande, W., & Larsson, M. 1996, Phys. Rev. A, 54, 3086
Sundström, G., et al. 1994, Science, 263, 785
Takano, S., et al. 1998, A&A., 329, 1156
Vigren, E., et al. 2008, Phys. Chem. Chem. Phys., 10, 4014
Vuitton, V., Yelle, R. V., & Anicich, V. G. 2006, ApJL, 647, 175
Vuitton, V., Yelle, R. V., & McEwan, M. J. 2007, Icarus, 191, 722
Wester, R., et al. 2002, J. Chem. Phys., 116, 7000
Woodall, J., Agúndez, M., Markwick-Kemper, A. J., & Millar, T. J. 2007, A&A, 466, 1197
Wu, H., & Glaser, R. 2005, Chem. Res. Toxicol., 18, 111
Zhaunerchyk, V., et al. 2007, Phys. Rev. Lett., 99, 013201